

Phase diagram and oxygen stoichiometry of Y-Ba-Cu-O thin films

K. Y. Yang, H. Homma,^{a)} R. Lee, R. Bhadra, M. Grimsditch, and S. D. Bader
Materials Science Division, Argonne National Laboratory, Argonne, Illinois 60439

J. P. Locquet and Y. Bruynseraede
Laboratorium voor Vaste Stof-Fysika en Magnetisme, Katholieke Universiteit Leuven, B-3030 Leuven, Belgium

Ivan K. Schuller
Physics Department, B-019, University of California, San Diego, La Jolla, California 92093

(Received 6 April 1988; accepted for publication 6 July 1988)

We have performed an exhaustive study of the phase diagram of Y-Ba-Cu-O thin films using chemical analysis, energy dispersive x-ray spectroscopy, Auger electron spectroscopy, and x-ray diffraction. We show that Raman scattering can provide information regarding impurity phases and oxygen stoichiometry in thin films

The mechanism responsible for superconductivity in high-temperature ceramic superconductors is one of the key issues in the field. A major difficulty with the study of physical phenomena in these materials is distinguishing purely physical properties from metallurgical and chemical effects such as microstructure, stoichiometry, homogeneity, and impurities. This is especially true in the case of thin films where many essential analysis techniques (such as neutron scattering) are not applicable and the neighborhood of foreign elements (the substrate) can also cause additional complications. On the other hand, a number of interesting problems can conveniently be addressed using thin films, for instance, the form of the excitation spectrum, Josephson or proximity type effects, and anisotropic properties of H_c or J_c . It is of considerable importance, therefore, to develop techniques which can help characterize the structural and chemical nature of thin films, especially with regards to the overall oxygen stoichiometry, the appearance of oxygen depleted zones, and the oxygen ordering. We have performed a detailed study of the phase diagram of Y-Ba-Cu-O thin films using conventional analysis techniques. More important, we show that Raman scattering can provide crucial information concerning impurity phases and in particular is able to determine the oxygen stoichiometry in thin films.

Before describing our work on thin films, it is convenient to briefly review the techniques commonly used for the characterization of the stoichiometry of high-temperature oxides and the difficulties encountered applying them to thin films. From the known amounts of each of the starting compounds used to fabricate the sample, if x rays or neutron scattering show the sample to be single phase, the metal ion stoichiometry can be determined. Additionally, if the impurity phases have been characterized, the precise location of the final composition in the phase diagram can be obtained. The absolute oxygen stoichiometry has only been determined on large bulk samples using sophisticated refinement techniques of neutron data,¹ although several techniques such as thermogravimetry² and oxygen evolution³ are useful in determining the relative oxygen stoichiometry (by com-

parison). X-ray diffraction can help determine the metal ion stoichiometry of sputtered or evaporated films if the rates from each of the targets are accurately known and if the impurity phases have been identified, although the oxygen stoichiometry and/or ordering cannot be determined using this technique. Chemical analysis (such as atomic emission spectroscopy) is reliable and able to give some information about the oxygen content but can only partially be applied to thin films due to the small amounts of material inherently available in this form. Again the precise oxygen stoichiometry and/or ordering remains elusive. Ion mill Auger electron spectroscopy (AES) can determine the relative concentration of atomic species although it is not clear what effect ion milling has on the oxygen concentration and it is quite insensitive to some elements such as yttrium. Moreover, being intrinsically a vacuum technique, the surfaces being analyzed may be enriched or depleted of oxygen or any other component (such as barium) and not be representative of the bulk material. Energy dispersive x-ray spectroscopy (EDX) is an accurate technique if a proper calibration sample is available and can be used on thin films. Although, in principle, oxygen concentrations can be detected, most commercial instruments are not equipped to detect the emissions from oxygen atoms. Here a calibration of the AES and EDX method was performed using "standard" samples that had been characterized by x-ray and neutron diffraction and chemical analysis. After calibration, all the above-mentioned techniques applied to a given thin-film sample yield values for the metal ion stoichiometry which agree to within a few percent.

In the fabrication of thin films, obtaining correct metal ion stoichiometry is, in principle, relatively simple since knowledge of the evaporation or sputtering rates enables films of the correct stoichiometry to be made. However, the partial oxygen pressure during evaporation, rate fluctuations, and the substrate temperature can seriously affect the sticking coefficients and alter the expected stoichiometry. The composition must then be verified using some of the techniques mentioned above, starting with the identification of impurity phases (if present) from conventional x-ray analysis.

^{a)} Present address: Department of Physics, Brooklyn College of City University of New York, Brooklyn, NY 11210.

Y-Ba-Cu-O thin films ($\sim 1 \mu\text{m}$) were prepared using a Riber molecular beam epitaxy (MBE) apparatus.⁴ The films were evaporated on rotating heated ($400\text{--}500^\circ\text{C}$) SrTiO_3 , ZrO_2 (9% Y), MgO , and Al_2O_3 substrates. Ba and Cu were evaporated from temperature-stabilized Knudsen cells, and Y was evaporated from an electron beam gun using electron impact emission spectroscopy (EIES) to stabilize typical rates of $4\text{--}5 \text{ \AA/s}$. Flowing oxygen was supplied close to the substrate surface, which raised the base pressure ($\sim 5 \times 10^{-11}$ Torr) to 2×10^{-6} Torr during evaporation. A number of annealing methods were attempted following recipes available in the published literature.⁵⁻⁷ The main idea behind all these annealing schedules is to allow sufficient time for the uptake and oxygen ordering to take place,^{8,9} together with the nucleation of a preferential growth orientation (texture or epitaxy), as well as to minimize the reactions with substrate. The annealing which gave the best results for our films (onset $T_c = 91 \text{ K}$, $\Delta T_c = 5 \text{ K}$) involves a 4 h anneal at 550°C , 1 h anneal at 650, 750, and 850°C each, followed by a 20°C/min cooling with a 1 h anneal at 500°C and a slow cool to room temperature.⁵

Testing the results of the various annealing schedules to find the one that produces the best sample is a cumbersome procedure, especially since, at certain temperatures and exposure times, unwanted secondary phases may be formed. We have found that Raman scattering provides an excellent speedy technique for the determination of secondary phases and perhaps more important the oxygen content. It has been reported in the literature that the strongest Raman line of $\text{YBa}_2\text{Cu}_3\text{O}_{7-\delta}$ at 500 cm^{-1} arises possibly from vibrations of oxygens located in the O_2 , O_3 , or O_4 sites.⁸⁻¹³ Figure 1 shows the dependence of the $\sim 500 \text{ cm}^{-1}$ Raman line on oxygen stoichiometry determined by a number of groups. The comparison of data implies that possibly the discrepancies arise mainly from the independent oxygen stoichiometry determination and not from a disagreement on the exact

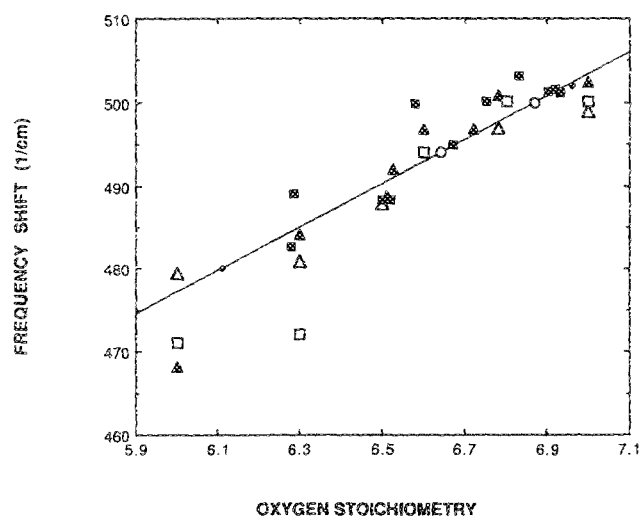


FIG. 1. Dependence of the $\sim 500 \text{ cm}^{-1}$ Raman line on oxygen stoichiometry determined by a number of groups: (■) from Ref. 9, (Δ) from Ref. 10, (\blacktriangle) from Ref. 11, (\blacklozenge) from Ref. 12, and (\square) from Ref. 13. Two thin-film samples before and after additional annealing are represented by (\circ). The solid line is a least squares fit to all the data.

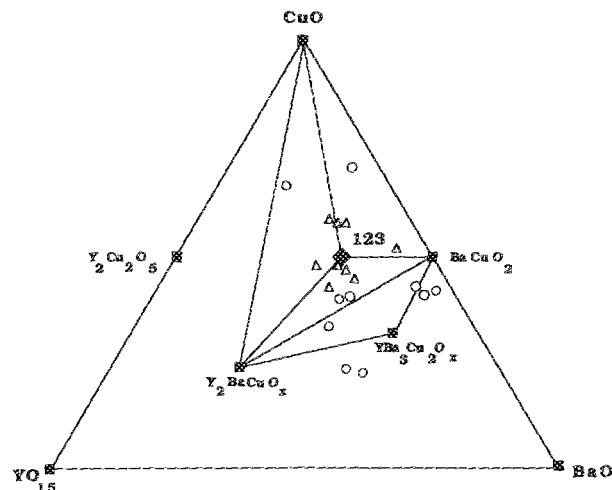


FIG. 2. Ternary phase diagram of thin-film Y-Ba-Cu-O projected onto a constant preparation plane: (■) known compounds, (Δ) superconducting samples, (\circ) not superconducting samples, (\blacklozenge) stoichiometric 1:2:3 compounds.

location of the Raman line. It is, therefore, expected that the relative error in the oxygen stoichiometry using Raman scattering is possibly better than what would be concluded from a naive examination of Fig. 1.

Figure 2 shows the ternary phase diagram of the Y-Ba-Cu-O films projected on a plane of constant preparation conditions (i.e., oxygen stoichiometry?) as determined by a combined wet chemistry, EDX, AES, and x-ray diffraction. As expected, the samples clustered around the 1:2:3 compound are superconducting, whereas the ones separated by phase boundaries are not. We should stress at this point that in order to obtain a reliable stoichiometry a number of calibrations using bulk samples and comparison from sample to sample had to be performed. This is particularly important to highlight since in many cases although the relative

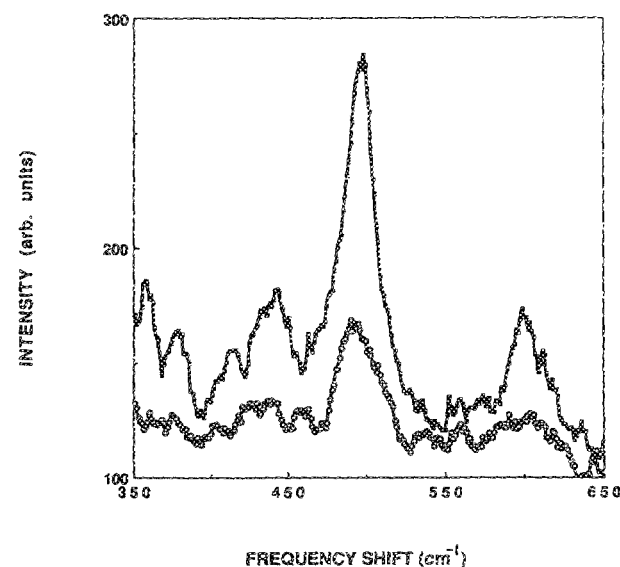


FIG. 3. Raman spectra of an $\text{YBa}_2\text{Cu}_3\text{O}_x$ thin film grown on SrTiO_3 substrate after a first anneal (upper) and after annealing at 450°C for 10 h (lower). Notice the shift on the Raman line at $\sim 500 \text{ cm}^{-1}$.

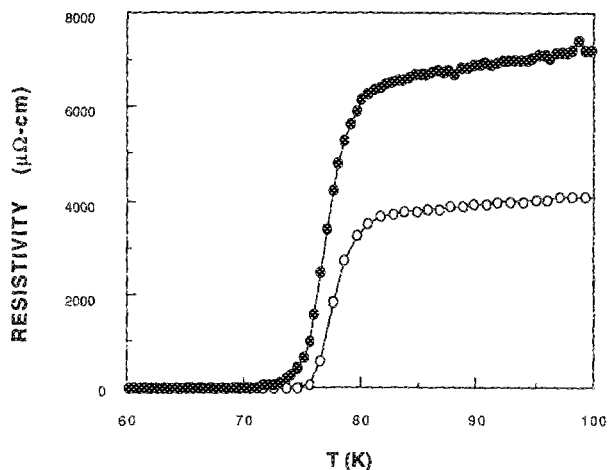


FIG. 4. Resistivity vs temperature for the sample shown in Fig. 3. The top curve (●) is for the first annealed sample and the lower one (○) after an additional anneal of 450 °C for 10 h. The Raman scattering data (Fig. 3) imply that oxygen concentrations correspond to $x \sim 6.64$ and $x \sim 6.87$ for the as-prepared and annealed samples, respectively.

numbers are quite accurate, in the absence of standards, the absolute stoichiometries could be considerably erroneous. For instance, the EDX results come from a semiquantitative analysis routine which does not take into account the oxygen bonding configuration of the metal ions.

Figure 3 shows Raman spectra from a film of 1:2:3 composition on SrTiO₃ substrates. The lower curve was taken for the sample after a first anneal, and it can be seen that the Raman line at $\sim 490 \text{ cm}^{-1}$ indicates a low oxygen content; the upper curve was taken after the sample had been reannealed at 450 °C for 10 h and the position of the Raman line shifted to $\sim 500 \text{ cm}^{-1}$ corresponding to a higher oxygen stoichiometry. (The line at $\sim 600 \text{ cm}^{-1}$ indicates that some second phase BaCuO₂ has also been produced during the annealing.) The oxygen stoichiometry extracted from the least-squares fit to all the data in Fig. 2 is $x \sim 6.64$ and 6.87 for the "first annealed" and reannealed samples, respectively.

Figure 4 shows a comparison of the resistivity of the YBa₂Cu₃O_{7- δ} thin films shown in Fig. 3. The onset of the transition (T_c) remains fixed whereas the zero resistance temperature (T_0) shifts to lower temperature for lower oxygen content. The broader transition is indicative of a lower average oxygen stoichiometry together with a broader oxygen stoichiometry distribution. The fact that the onset of the transition remains fixed whereas the zero resistance drops indicates that in this case the sample characteristics change due to the presence of a smaller superconducting fraction leading to a decoupling of superconducting phases of the various ceramic grains. Since Raman scattering averages over a finite volume of the sample, it cannot distinguish between changes due to a phase decoupling or an overall lowering of the magnitude of the superconducting order parameter. The midpoints of the transition, extracted from the experimental relationship between oxygen stoichiometry and transition temperatures in bulk samples,^{12,14} are in good quantitative agreement with the values obtained from the Raman data.

The behavior described above has been observed systematically in a large number of samples, indicating that Raman scattering is a powerful diagnostic tool for the characterization of high-temperature oxide superconducting films. Clearly, as Fig. 3 shows, there is a need to increase the precision of the Raman data versus oxygen stoichiometry in order to allow a more exact determination of oxygen stoichiometry.

In summary, we have determined the phase diagram of thin-film YBa₂Cu₃O_{7- δ} ceramic superconductors. The results show that EDX, wet chemistry, AES, and x-ray diffraction together with bulk standards allow a precise determination of the metal ion stoichiometry. We have also found that Raman scattering is a powerful tool which can be used for the determination of impurity phases and oxygen stoichiometry.

This work was supported by the U.S. Department of Energy, BES-Materials Sciences under contract No. W-31-109-ENG38 (at ANL), the National Science Foundation under grant No. DMR-8803185, Office of Naval Research grant N0014-88-0480 (at UCSD), and the Belgian Interuniversity Institute for Nuclear Science (I.I.K.W.). International travel was provided by NATO grant RG-85/0695 and the Belgian National Science Foundation.

¹J. Jorgensen, M. A. Beno, D. G. Hinks, L. Soderholm, K. J. Volin, R. L. Hitterman, J. D. Grace, and Ivan K. Schuller, *Phys. Rev. B* **36**, 3608 (1987).

²See, for instance, J. M. Tarascon, W. R. McKinnon, H. L. Green, G. W. Hull, and E. M. Vogel, *Phys. Rev. B* **36**, 226 (1987).

³H. Strauven, J.-P. Locquet, Q. B. Verbeke, and Y. Bruynseraede, *Solid State Commun.* **65**, 293 (1988); also see Proceedings of the Conference on High Temperature Superconductivity and Materials and Mechanisms of Superconductivity (Interlaken, Switzerland, in press).

⁴K. Y. Yang, H. Homma, R. Lee, R. Bhadra, J.-P. Locquet, Y. Bruynseraede, and Ivan K. Schuller, *Proc. MRS Spring Meeting, EA-14*, p. 357 (1988).

⁵M. Naito, R. H. Hammond, B. Oh, M. R. Hahn, J. W. P. Hsu, P. Rosenthal, A. F. Marshall, M. R. Beasley, T. H. Geballe, and A. Kapitulnik, *J. Mater. Res.* **2**, 713 (1987).

⁶P. Chaudhari, R. H. Koch, R. B. Laibowitz, T. R. McGuire, and R. J. Gambino, *Phys. Rev. Lett.* **58**, 2684 (1987).

⁷J. Kwo, T. C. Hsieh, R. M. Fleming, M. Hong, S. H. Liou, B. A. Davidson, and L. C. Feldman, *Phys. Rev. B* **36**, 4039 (1987).

⁸Ivan K. Schuller, D. G. Hinks, M. A. Beno, D. W. Capone II, L. Soderholm, J.-P. Locquet, Y. Bruynseraede, C. U. Segre, and K. Zhang, *Solid State Commun.* **63**, 385 (1987).

⁹R. Bhadra, T. O. Brun, M. A. Beno, B. Dabrowski, D. G. Hinks, J. Z. Liu, J. D. Jorgensen, L. J. Nowicki, A. P. Paulikas, Ivan K. Schuller, C. U. Segre, L. Soderholm, B. Veal, H. H. Wang, J. M. Williams, K. Zhang, and M. Grimsditch, *Phys. Rev. B* **37**, 5142 (1988).

¹⁰C. Thomsen, R. Liu, M. Bauer, A. Wittlin, L. Genzel, M. Cardona, E. Schönher, W. Bauhofer, and W. König, *Solid State Commun.* **65**, 55 (1988).

¹¹G. A. Kourouklis, A. Jayaraman, B. Batlogg, R. J. Cava, M. Stavola, D. M. Krol, E. A. Rietman, and L. F. Schneemeyer, *Phys. Rev. B* **36**, 8320 (1987).

¹²Y. Dai, J. S. Swinnea, H. Steinfiink, J. B. Goodenough, and A. Champion, *J. Am. Chem. Soc.* **109**, 5291 (1987).

¹³D. Kirillov, J. P. Collman, J. T. McDevitt, G. T. Yee, M. J. Holcomb, and I. Bozovic, *Phys. Rev. B* **37**, 3660 (1988).

¹⁴See, for instance, W. K. Kwok, G. W. Crabtree, A. Umezawa, B. W. Veal, J. D. Jorgensen, S. K. Malik, L. J. Nowicki, A. P. Paulikas, and L. Nunes, *Phys. Rev. B* **37**, 106 (1988).